Journal of Alloys and Compounds 508 (2010) 200–205

Contents lists available at ScienceDirect

Journal of Alloys and Compounds

journal homepage: www.elsevier.com/locate/jallcom

Influence of sulfate ions on properties of co-precipitated $Y_3Al_5O_{12}:Nd^{3+}$ nanopowders

T.G. Deineka[a], A.G. Doroshenko[a], P.V. Mateychenko[a], A.V. Tolmachev[a], E.A. Vovk[a], O.M. Vovk[a], R.P. Yavetskiy[a,*], V.N. Baumer[b], D.S. Sofronov[b]

[a] Institute for Single Crystals, STC "Institute for Single Crystals", NAS of Ukraine, 60 Lenin Ave., 61001 Kharkov, Ukraine
[b] SSI STC "Institute for Single Crystals" NAS of Ukraine, 60 Lenin Ave., 61001 Kharkov, Ukraine

ARTICLE INFO

Article history:
Received 26 May 2010
Received in revised form 3 August 2010
Accepted 4 August 2010
Available online 19 August 2010

Keywords:
YAG
Co-precipitation
Dispersant
Optical ceramics

ABSTRACT

A new precursor of yttrium aluminum garnet with an approximate composition of $NH_4AlY_{0.6}(CO_3)_x(OH)_y(SO_4)_z{\cdot}nH_2O$ has been synthesized via a reverse strike co-precipitation method with ammonium hydrogen carbonate as the precipitant and ammonium aluminum sulfate as the sulfate ions source. The evolution of phase, chemical composition and morphology of the precursor during calcination has been studied by means of XRD, XPS, DTA–TG, BET methods and FT-IR spectroscopy. The loosely agglomerated powders with narrow size distribution, spherical shapes and diameter of 50–60 nm have been obtained by calcination of the sulfate-containing precursor at 1100 °C for 2 h. The doping by sulfate ions enhances densification of $Y_3Al_5O_{12}:Nd^{3+}$ nanopowders compared to undoped ones. This leads to improved microstructure and optical transmittance of vacuum sintered ceramics prepared from sulfate-doped nanopowders.

1. Introduction

Synthesis of well-dispersed nanocrystalline powders is a key factor in advanced technologies of transparent ceramics fabrication. Nanopowders provide more homogenous particle packing during molding and densify into transparent bodies without applying a pressure at lower temperatures compared to conventional micron-sized powders. To produce highly transparent ceramics which optical and laser characteristics are comparable with corresponding single crystals the initial nanopowders should meet following requirements: low agglomeration degree, spherical shape, ultrafine particle size (near 100 nm) and narrow size distribution [1,2]. Nowadays relatively simple wet chemical methods are widely used to synthesize oxide nanopowders of multication compounds due to excellent mixing of starting materials and homogeneity of final product at the molecular level. For instance, co-precipitation from water solutions with subsequent calcination of amorphous precipitant to convert it into crystalline phase is considered as one of the most promising methods to produce $Y_3Al_5O_{12}$ (YAG) nanopowders ([3–7] and references therein). Sinterability of nanopowders heavily depends on chemical composition and physico-chemical properties of the precursor. Co-precipitation with ammonium hydrogen carbonate (AHC) usually leads to formation of carbonate precursors, which decompose at low temperatures and possess only loose agglomeration. The favorable morphological features of precursors are responsible for creation of low agglomerated oxide nanopowders by calcination. The advantages of carbonate precursors for production of highly sinterable nanopowders were disclosed for rare earth sesquioxides and YAG. In [6] it was shown that YAG nanopowders obtained from carbonate precursor with composition of $NH_4AlY_{0.6}(CO_3)_x(OH)_y{\cdot}nH_2O$ densify more homogenously and achieve higher density after vacuum sintering compared to the powders obtained from hydroxide precursor. At the same time, even low residual agglomeration of carbonate-derived YAG nanopowders impedes formation of transparent ceramics appreciably and requires additional technological treatment of resulting nanopowders, such as special drying, wet or dry high-energy ball milling, etc. For this reason so-called "design" of nanopowders is an extremely important challenge of advanced powder technologies.

The control of morphological and physico-chemical properties of oxide nanopowders can be achieved via utilization of additives modifying in some way the charge state of particle surfaces. The purpose of modification is to provide formation of double charged layer on the surface of each particle and, consequently, to increase the repulsion forces between the particles and prevent their agglomeration. Recently it was shown that introduction of sulfate ions into reaction mixture allows one to produce

* Corresponding author at: Institute for Single Crystals, STC "Institute for Single Crystals", NAS of Ukraine, Department of Complex Crystalline Materials, 60 Lenin Ave., 61001 Kharkov, Ukraine. Tel.: +380 57 341 0415; fax: +380 57 340 9343.
E-mail address: yavetskiy@isc.kharkov.ua (R.P. Yavetskiy).

0925-8388/$ – see front matter © 2010 Elsevier B.V. All rights reserved.
doi:10.1016/j.jallcom.2010.08.046

low agglomerated Al_2O_3 [8], Sc_2O_3 [1] and Y_2O_3 [9–11] powders with spherical morphology. It was reported that sulfate ions promote formation of monodisperse spherical nanosized powders and hinder them from agglomeration. The doping by the sulfate ions can be realized in several ways when ammonium sulfate $(NH_4)_2SO_4$ is used as sulfate ions source. $(NH_4)_2SO_4$ can be added into reaction mixture during precipitation [3–5], during aging [10,11], or resulting precipitant can be rinsed by $(NH_4)_2SO_4$ solution [9]. The addition of the ammonium sulfate directly into reaction mixture gives rise to local change of mixture pH value and consequently to local variations of chemical composition of resulted powders [5]. The introduction of sulfate ions during aging or by precipitant rinsing by $(NH_4)_2SO_4$ solution does not permit to control the concentration of sulfates in the precursor. In the present work we use double crystallized aluminum ammonium sulfate $Al(NH_4)(SO_4)_2{\cdot}12H_2O$ as the aluminum and sulfate ions sources.

The studies of the sulfate ions influence on nanopowders properties are mainly done on rare earth sesquioxides Sc_2O_3 and Y_2O_3. Despite some works report that doping by sulfate ions improves structural and morphological characteristics of YAG nanopowders [2,5,12,13], the role of sulfate ions in the production of highly sinterable YAG nanopowders is not clear. The purpose of this work is to study the influence of sulfate ions on the morphology, size, agglomeration degree and sintering peculiarities of carbonate-derived YAG nanopowders.

2. Experimental

2.1. Synthesis

YAG:Nd^{3+} nanopowders (3 at.%) were produced by a reverse strike co-precipitation method. The yttrium and neodymium nitrates were used as starting materials. The ammonium aluminum sulfate $Al(NH_4)(SO_4)_2{\cdot}12H_2O$ (special purity grade) was utilized as the aluminum and sulfate ions source. Nitrates were prepared by dissolving of Y_2O_3 and Nd_2O_3 (both of special purity grade) in concentrated nitric acid with subsequent evaporation of acid excess. The 1 M ammonium hydrogen carbonate NH_4HCO_3 was used as a precipitant. The concentrations of $Y(NO_3)_3$, $Nd(NO_3)_3$ and $Al(NH_4)(SO_4)_2{\cdot}12H_2O$ solutions were 0.5 M. The precipitation was carried out at the room temperature; the drip rate was 2 ml/min. The resultant suspension was aged for 24 h and then filtered via suction filtration. After repeated washing with ethanol and deionized water the precipitant was dried at 100 °C for 24 h. YAG:Nd^{3+} nanopowders of different dispersion were obtained by precursor calcination in 900–1300 °C temperature range for 2 h in the air atmosphere. YAG:Nd^{3+} nanopowders for vacuum sintering were molded by uniaxial pressing method with a pressure of 200 MPa. The sintering of green bodies was performed using vacuum furnace with tungsten heating elements at the temperature of 1800 °C and vacuum of 10^{-3} Pa without sintering aids.

2.2. Characterization

Differential thermal and thermogravimetrical analyses of precursor were carried out using a MOM Q-1500D derivatograph (Hungary). The heating rate was 10 °C/min, the alpha alumina was used as a reference. For thermal analysis the precursor was dried at the room temperature. Fourier transform infrared (FT-IR) spectra of the samples were measured on a FT-IR spectrometer SPECTRUM ONE (PerkinElmer) with the KBr pellet. Phase identification was performed via X-ray diffraction (XRD) method with a SIEMENS D-500 X-ray diffractometer using nickel filtered Cu K_α radiation. The phases were identified using "PDF-4" card file and "EVA" retrieval system, included in the diffractometer software. Specific surface area of the powders was determined by BET (Brunauer–Emmett–Teller) method. Morphology of the powders was observed by a transmission electronic microscope TEM-125 operated at 100 kV accelerating voltage. Before microscopic examination, the powders were subjected to ultrasonication by using an ultrasonic dispergator UZDN-A at frequency of 22 kHz for 45 s. The distilled water was used as a working medium. The sulfur content was determined by X-ray photoelectron spectroscopy (XPS) method by a XSAM-800 Kratos spectrometer using Mg K_α radiation, and by electron probe microanalysis using a Jeol JSM-6390LV (Jeol) scanning electron microscope with INCA 350 microanalysis system. The density of ceramic samples was determined by Archimedes method. The microstructure of ceramics was observed by a Jeol JSM-6390LV (Jeol) scanning electron microscope after thermal etching at $T = 1500$ °C for 2 h.

3. Results and discussion

3.1. The effect of precipitant

Co-precipitation of inorganic mother salts by AHC leads to the following hydrolysis reaction of AHC [6]:

$$NH_4HCO_3 + H_2O \Leftrightarrow NH_4OH + H_2CO_3 \quad (1)$$

$$NH_4OH \Leftrightarrow NH_4^+ + OH^- \quad (2)$$

$$H_2CO_3 \Leftrightarrow H^+ + HCO^{3-} \quad (3)$$

$$HCO_3^- \Leftrightarrow H^+ + CO_3^{2-} \quad (4)$$

According to Eqs. (1)–(4), OH^- and CO_3^{2-} anions act as the precipitating ions. Thus, the chemical composition of a formed precursor is a result of completion between these anions and metal cations (Y^{3+}, Al^{3+}) during precipitation. As one can see, the obtained precursor is usually a carbonate compound, which is only softly agglomerated and has low decomposition temperature. It is known that precipitation of Al^{3+} by AHC leads to formation of AlOOH or $NH_4Al(OH_2)CO_3$, whereas interaction of Y^{3+} with AHC results in formation of normal or basic carbonates of $Y_2(CO_3)_3{\cdot}nH_2O$ or $Y(OH)CO_3$, correspondingly. The aluminum rich precursor is formed first and is then coated by yttrium enriched particles during precipitation process. For this reason precise control of the precipitation parameters is required to obtain YAG nanopowders of stoichiometric composition. The SO_4^{2-} ions have drastic effect on precursor composition due to their strong tendency to form complexes. The influence of SO_4^{2-} on the precursor composition and YAG nanopowders properties is presented below.

3.2. DTA–TG analysis

The thermal decomposition curves of YAG:Nd^{3+} precursor are given in Fig. 1. Continuous mass loss of the sample is observed up to 1200 °C and is accompanied by total weight loss of 54%. Three steps can be distinguished on the thermogravimetric curve in 20–200, 200–900 and 900–1200 °C temperature ranges, indicating step-wise decomposition of the precursor. The most intensive weight loss of 31% is observed at the first stage, following by two relatively sloping stages. The corresponding mass losses are 17 and 6%. The ignition loss observed up to 200 °C is caused mainly by removal of molecular and hydrated water. In the temperature range of 200–900 °C the dehydroxylization and carbonate decomposition occur, while desulfurization takes place up to 1200 °C. The exothermic effect on the DTA curve at 900–1000 °C was assigned to garnet phase formation.

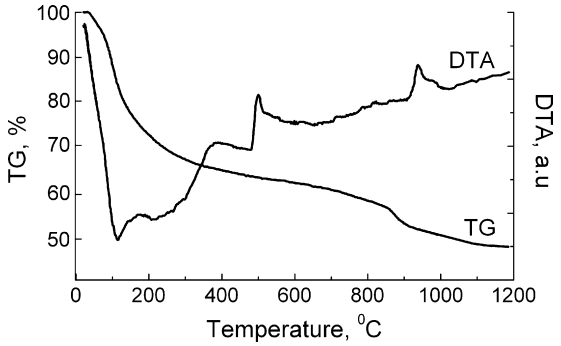

Fig. 1. DTA and TG curves of the precursor.

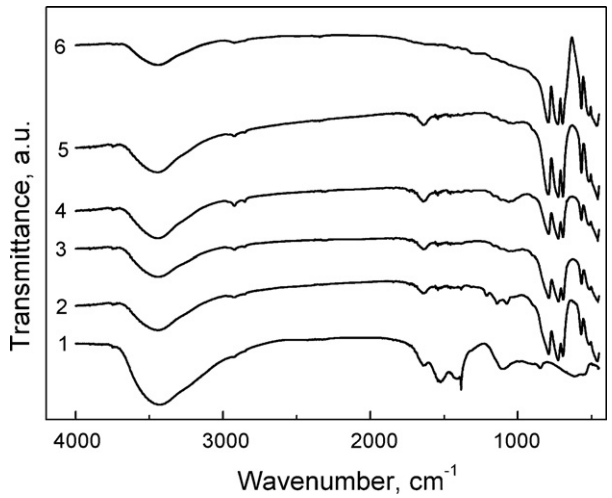

Fig. 2. FT-IR spectra of precursor (1) and YAG:Nd^{3+} nanopowders calcined at 900 °C (2); 1000 °C (3); 1100 °C (4); 1200 °C (5) and 1300 °C (6).

3.3. FT-IR spectra

FT-IR spectra of precursor and its calcination products are presented in Fig. 2. The wide structureless band with a maximum at 3435 cm^{-1} corresponds to absorption of molecular water (~3200–3500 cm^{-1}) as well as free hydroxyl groups (~3200–3500 cm^{-1}) [14]. The broad peak at ~1640 cm^{-1} is characteristic to H–O–H bending mode of molecular water. The strong absorption bands in 975–1230 cm^{-1} range correspond to SO_4^{2-}. It is known that SO_4^{2-} ions demonstrate characteristic absorption bands in the 1040–1210 cm^{-1} range and the range may be extended if the bands are split [14]. The intense peaks at 520 and 1385 cm^{-1} indicate the presence of residual NH^{4+} and NO^{3-} groups in the precursor [13]. The wide absorption bands at 1520 and 1410 cm^{-1} were assigned to asymmetric stretch of C–O band in CO_3^{2-}, while the peak at 845 cm^{-1} was attributed to deformational vibration of C–O in CO_3^{2-}, respectively. Calcination of precursor at T = 900 °C significantly decreases the band intensities of molecular water, free hydroxyls and carbonate groups, but does not influence those of sulfate ions (Fig. 2). Thus, at the temperatures up to 900 °C gradual dehydration and carbonate decomposition mainly occur, while desulfurization takes place at higher temperatures. The sample calcined at T = 900 °C demonstrates the characteristic absorption bands in 400–800 cm^{-1} wavelength range, corresponding to Y–O, Al–O and Y–Al–O stretching vibrations [13,15]. This indicates the formation of garnet phase after final precursor decarbonization. The violent desulfurization of nanopowders occurs in 900–1200 °C temperature range in good agreement with DTA–TG data (Fig. 1). The complete removal of sulfate ions registered after calcination at 1300 °C, is accompanied by disappearing of absorption bands in 1040–1210 cm^{-1} range. The weak residual absorption peaks in the calcined samples (1300 °C) are connected probably with H_2O adsorbed onto powder surface in the air.

3.4. Precursor composition

Co-precipitation of yttrium and aluminum nitrates by AHC results in formation of complex precursor with the approximate composition of $NH_4AlY_{0.6}(CO_3)_x(OH)_y{\cdot}nH_2O$ [6,12]. Our DTA data (Fig. 1) agree well with that reported for carbonate precursor [6,7]. However, TG shows that our precursor has higher decomposition temperature (the observed difference is of about 200 °C). Usually sulfate-doped precipitates demonstrate higher thermal stability compared to undoped ones [1]. According to FT-IR data the mass loss in the temperature range of 900–1200 °C corresponds to nanopowders desulfurization indicating that precursor contains sulfate ions. The concentration of sulfate ions was determined by XPS and electron probe microanalysis methods. According to electron probe microanalysis the precursor contains 2.7 at.% of sulfur. The calcination temperature increase from 900 to 1100 °C results in sulfur concentrations decrease from 1.13 to 0.16 at.%. The final removal of sulfate ions (below the analyzer sensitivity limit of 0.1 at.%) occurs after powders calcination at 1200 °C. The XPS data evidences, that sulfur ions form SO_4^{2-} anions in the precursor as well as in calcined YAG nanopowders, since bonding energy value of sulfur 2s-shell (232.3 eV) corresponds to well-known data for $MeSO_4$ compounds. Hence the new precursor with approximately composition of $NH_4AlY_{0.6}(CO_3)_x(OH)_y(SO_4)_z{\cdot}nH_2O$ was obtained by co-precipitation method. Formation of precursors containing sulfate ions by wet chemical methods was also reported in [5].

3.5. XRD analysis

Evolution of the precursor phase composition during calcination is given in Fig. 3. The initial precursor as well as the powders cal-

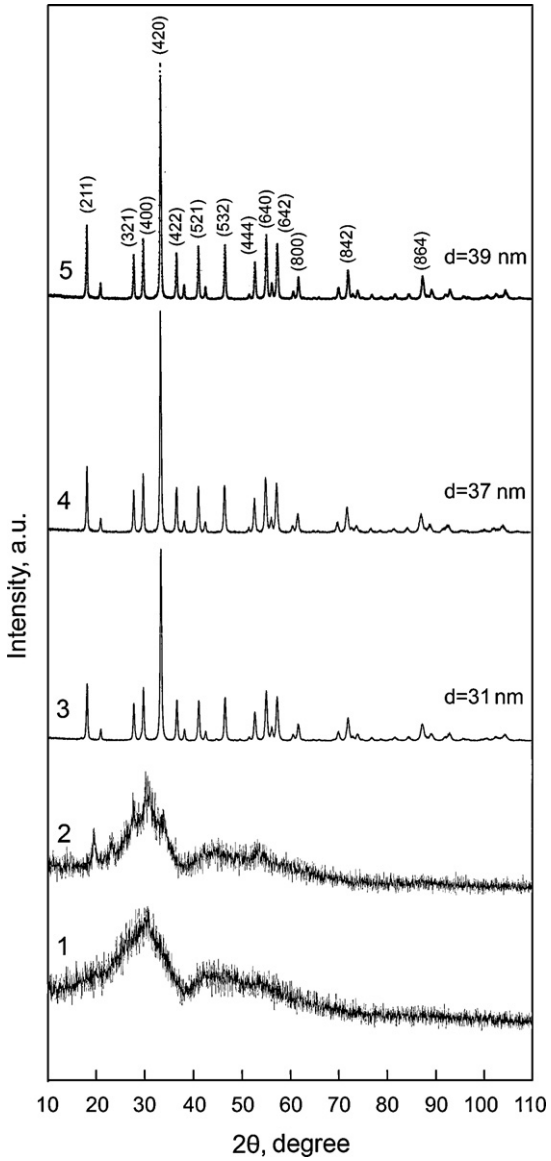

Fig. 3. XRD spectra of YAG:Nd^{3+} nanopowders calcined at 500 °C (1); 800 °C (2); 900 °C (3); 1000 °C (4) and 1100 °C (5).

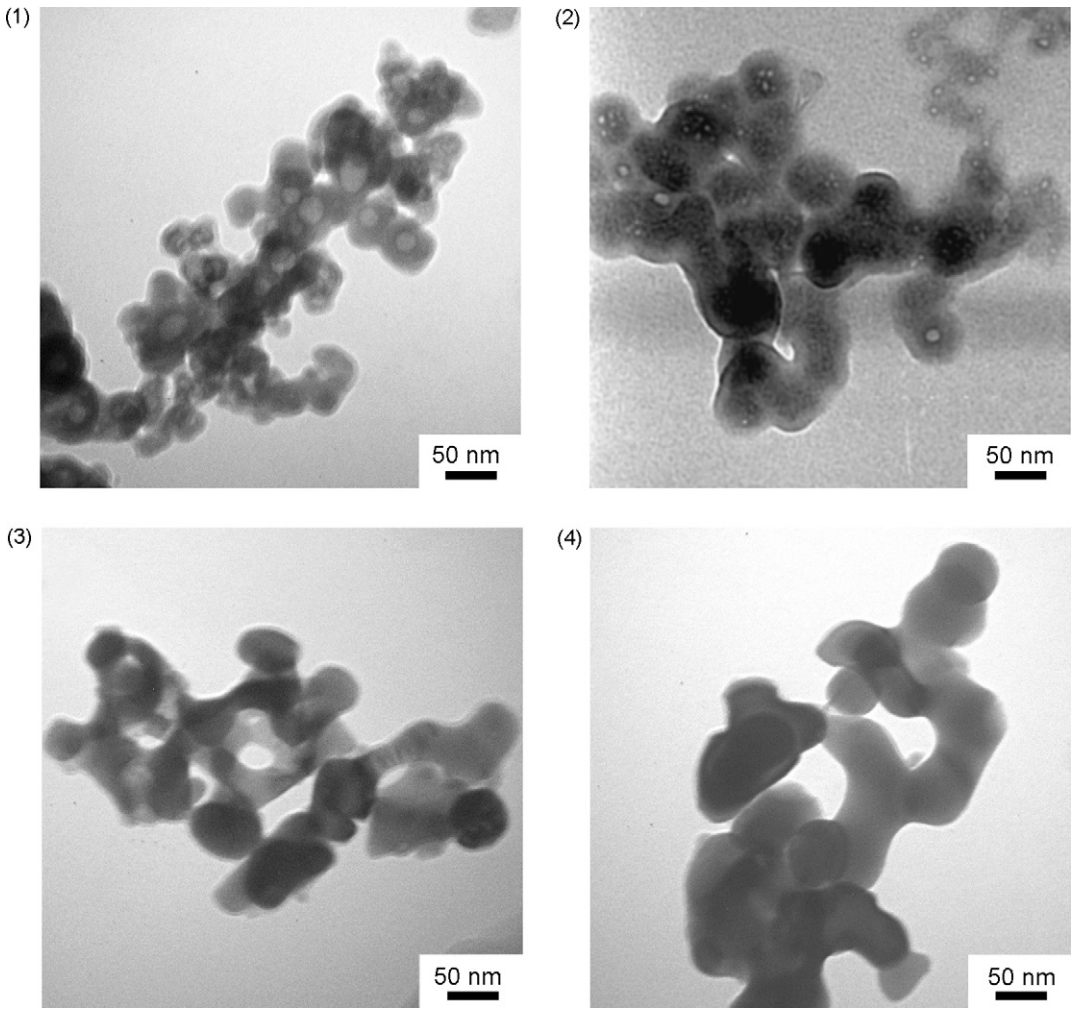

Fig. 4. The morphology of the precursor (1) and YAG:Nd^{3+} nanopowders calcined at $T = 900\,^{\circ}C$ (2); $T = 1100\,^{\circ}C$ (3); $T = 1200\,^{\circ}C$ (4) and $T = 1300\,^{\circ}C$ (5).

cined below 900 °C was amorphous. YAG phase formation occurs at $T = 900\,^{\circ}C$. The powders calcined at 900 °C and above this temperature are single-phase since all diffraction peaks correspond to YAG crystal lattice (Fig. 3). The formation temperature of garnet phase during $NH_4AlY_{0.6}(CO_3)_x(OH)_y(SO_4)_z{\cdot}nH_2O$ precursor thermolysis is in accordance with that for carbonate precursor [6,7], thus sulfate ions do not influence the phase formation temperatures and their sequence. As the calcination temperature rises, the diffraction peaks become more and more intense and narrow, evidencing the average crystallite size increase. However, this increase is very weak (Fig. 3), indicating that sulfate ions slow down the diffusion mass transport.

FT-IR, TG and electron probe microanalysis show that YAG desulfurization occurs till the temperature of 1300 °C, while single-phase YAG forms after calcination at $T = 900\,^{\circ}C$. According to XPS data residual sulfate ions create SO_4^{2-} anions, so YAG powders are doped by SO_4^{2-}-ions in 900–1300 °C temperature range. We suppose two possibilities of such a doping. First, SO_4^{2-}-ions can be a part of impurity phases like $Y_2(SO_4)_3$, $Y_2O_2SO_4$ or $Al_2(SO_4)_3$ in the concentration below the XRD detection limit (1 mass%). Secondly, since YAG nanopowders have high specific surface area, SO_4^{2-} can enter into surface layers of YAG lattice. For beryllium oxide obtained by thermal decomposition of beryllium sulfate it was shown, that residual SO_4^{2-} ions can be located in the bulk or the surface layers of BeO prior to dissociation [16]. Since the radius of SO_4^{2-} anion (~2.3 Å) [17] is much higher than that for oxygen ion (1.24 Å), and assuming that every nanoparticle is a single crystal, SO_4^{2-} entering into the particle volume is highly unlikely. So we suppose that SO_4^{2-} in YAG nanopowders is placed at the nanoparticles surface.

3.6. Powder morphology

The morphology of precursor and YAG:Nd^{3+} nanocrystalline powders is shown in Fig. 4. The precursor consists of spherical well-dispersed particles with an average diameter of 10–30 nm. Sulfate ions adsorbed onto the precursor surface form double electric layer (electric stabilization), which increases repulsion forces between the particles and improves precursor dispersion. YAG:Nd^{3+} nanoparticles obtained by precursor calcination inherit

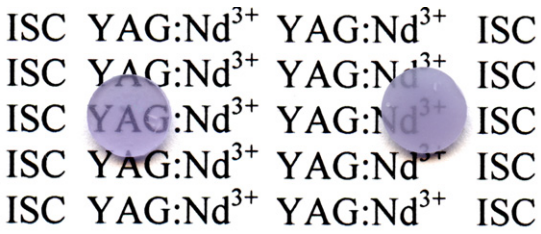

Fig. 5. YAG:Nd^{3+} (3 at.%) ceramics obtained by vacuum sintering at 1800 °C for 10 h using sulfate-doped (1) or undoped (2) nanopowders calcined at $T = 1100\,^{\circ}C$ for 2 h. The samples thickness is 1 mm.

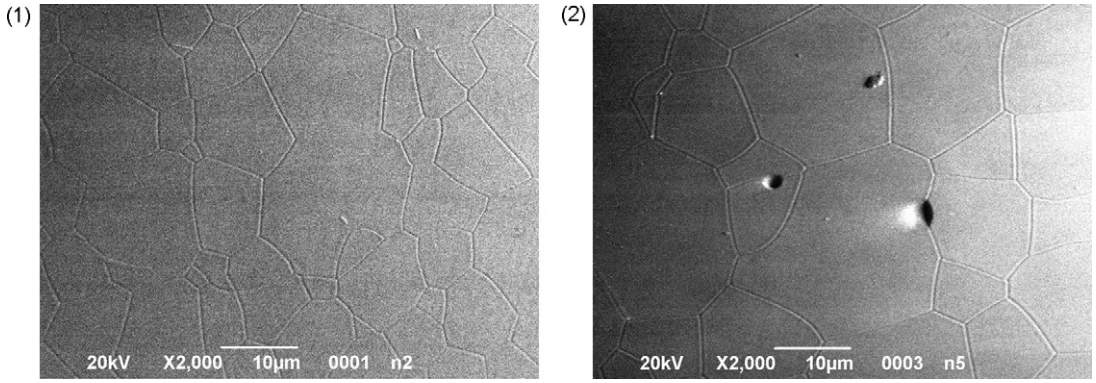

Fig. 6. SEM micrograph of surfaces of YAG:Nd^{3+} (3 at.%) ceramics, obtained by vacuum sintering of sulfate ions doped (1) and undoped (2) nanopowders calcined at T = 1100 °C for 2 h.

the morphology of precursor (memory shape effect). For instance, calcination at 1100 °C for 2 h leads to creation of well-dispersed uniform spherical particles of 50–60 nm in diameter (Fig. 4, 2). The particle diameter calculated by BET method (60 nm) perfectly matches with that determined by TEM, indicating low agglomeration degree of the powders. The calcination temperature increase results in formation of contact necks between some of the particles while the spherical morphology remains unaltered (Fig. 4, 3). Further temperature increase up to 1300 °C results in inconvertible morphology changes. Along with average particle size increase the formation of coral-like hard aggregates occurs as a consequence of significant rise of diffusion mass transport (Fig. 4, 4). It should be noted that morphology of YAG particles correlates with their calcination temperature (or with concentration of residual sulfate ions). Only nanopowders containing more than 0.1 at.% of sulfate ions demonstrate spherical morphology of particles.

The doping by sulfate ions is favorable for the spherical morphology and excellent dispersion of precursor and calcined YAG:Nd^{3+} nanopowders. First, the free SO_4^{2-}-ions act as a much stronger coagulant compared to NO_3^--ions, probably, due to higher valence state [1]. This leads to production of well-dispersed precursor. Moreover, the residual sulfate ions can reduce crystal anisotropy among crystal planes of YAG:Nd^{3+} during calcination, as recently was observed for Y_2O_3 [10,11]. This provides equal growth rate of different crystallographic planes of YAG:Nd^{3+} during recrystallization leading to near monodisperse particle size distribution. The increase of decomposition temperature of sulfate-containing precursor results in decrease of diffusion mass transport between the particles, improving their dispersion.

3.7. Sintering of YAG:Nd^{3+} nanopowders

It is known that microstructure and optical transmittance of sintered ceramics is highly influenced by the nanopowders properties, namely average particle size, morphology, particle size distribution and agglomeration degree. The effect of sulfate ions doping on sintering of YAG:Nd^{3+} nanopowders was studied via comparison of morphological and optical characteristics of vacuum sintered ceramics. The vacuum sintering was conducted at 1800 °C for 10 h using furnace equipped with tungsten heaters. Undoped YAG:Nd^{3+} nanopowders obtained according to [7] were used for purposes of comparison. Both powders were calcined at T = 1100 °C during 2 h and compacted in one batch by cold uniaxial pressing method. The densities of obtained green bodies were ranged within 45–50% limit. The polished samples of ceramics obtained using sulfate-doped and undoped YAG:Nd^{3+} nanopowders are presented in Fig. 5. The densities of ceramics were 99.8–99.9% after vacuum sintering. Despite non-optimized compaction and sintering conditions, both powders densify into translucent YAG:Nd^{3+} ceramics – the text can be read through the 1 mm thick samples. Fig. 5 shows that ceramics obtained with sulfate-doped YAG:Nd^{3+} nanopowders have better optical transmittance compared to that prepared from undoped powders. This fact arises from the better dispersion of sulfate ions doped YAG nanopowders.

The microstructure of YAG:Nd^{3+} ceramics obtained using sulfate-doped and undoped nanopowders is given in Fig. 6. The samples have equal crystallite sizes of 10–15 mkm as determined by the linear intercept method from 100 randomly selected grains. The only difference between two samples is lower porosity of the ceramics obtained using sulfate-doped precursor of $NH_4AlY_{0.6}(CO_3)_x(OH)_y(SO_4)_z{\cdot}nH_2O$ composition (Fig. 6.1). The numerous literature data suggest that sulfate ions influence sintering process via more homogenous densification of nanopowders, as well as via more complete pore removal [10,11]. This leads to improved structural and morphological characteristics of ceramics and higher transparency (Fig. 5,6). Thus sulfate ions affect not only morphology of nanopowders, but also their sinterability. Obviously, some residual sulfate ions can survive in ceramics after vacuum sintering. However their concentration is below detection limit of XPS and electron probe microanalysis methods. One can suppose that residual SO_4^{2-} form liquid phase during sintering, accelerating formation of pore free ceramics, as it was reported for Y_2O_3 [11]. But to confirm this hypothesis additional research is needed. Obtaining the transparent ceramics without any sintering aids is a purpose of our further studies.

4. Conclusions

The new $Y_3Al_5O_{12}$ precursor with an approximate composition of $NH_4AlY_{0.6}(CO_3)_x(OH)_y(SO_4)_z{\cdot}nH_2O$ has been synthesized by the co-precipitation method using ammonium hydrogen carbonate as the precipitant and aluminum ammonium sulfate as the sulfate ions source. The influence of sulfate ions on the morphology, dispersion and sinterability of $Y_3Al_5O_{12}$:Nd^{3+} nanopowders calcined in 800–1200 °C temperature range has been studied. It has been shown that sulfate ions adsorbed onto the particles surface form double electric layer, which increases interparticle repulsion forces and improves precursor dispersion. The calcination of the precursor at 1100 °C for 2 h result in formation of $Y_3Al_5O_{12}$:Nd^{3+} near monodisperse spherical particles of 50–60 nm in diameter possessing only lose agglomeration. $Y_3Al_5O_{12}$:Nd^{3+} nanopowders prepared from sulfate-containing precursor have better sinterability compared with conventional carbonate-derived powders therefore $Y_3Al_5O_{12}$:Nd^{3+} vacuum sintered ceramics demonstrates higher transmittance and lower residual porosity.

Acknowledgments

The work was supported by NAS of Ukraine through the departmental academic Project "Kalibr" (2007–2009). The XPS spectra measurements by Dr. M.V. Dobrotvorskaya and experimental assistance by group of Prof. L.A. Litvinov are greatly acknowledged.

References

[1] J.-G. Li, T. Ikegami, T. Mori, Y. Yajima, J. Am. Ceram. Soc. 87 (2004) 1008–1013.
[2] Yu.L. Kopylov, V.B. Kravchenko, S.N. Bagayev, V.V. Shemet, A.A. Komarov, O.V. Karban, A.A. Kaminskii, Opt. Mater. 31 (2009) 707–710.
[3] Pat. 10101333 (A) Japan, IC[1–7] C04B 35/44; C01F 17/00; H01S 3/16, T. Yanagitani, H. Yagi, M. Ichikawa, Publ. 21.04.98.
[4] Pat. 10101411 (A) Japan, IC[1–7] C04B 35/44; C01F 17/00, T. Yanagitani, H. Yagi, Y. Hiro, Publ. 21.04.98.
[5] N. Matsushita, N. Tsuchiya, K. Nakatsuka, T. Yanagitani, J. Am. Ceram. Soc. 82 (1999) 1977–1984.
[6] J.-G. Li, T. Ikegami, J. Lee, T. Mori, Y. Yajima, J. Eur. Ceram. Soc. 20 (2000) 2395–2405.
[7] V.N. Baumer, E.A. Vovk, O.M. Vovk, T.G. Deineka, M.B. Kosmyna, P.V. Mateychenko, V.M. Puzikov, Z.P. Sergienko, A.V. Tolmachev, A.N. Shekhovtsov, R.P. Yavetskiy, Funct. Mater. 15 (2008) 540–545.
[8] M.D. Sacks, T.-Y. Tseng, S.Y. Lee, Ceram. Bull. 63 (1984) 301–310.
[9] N. Saito, Shin-ichi Matsuda, T. Ikegami, J. Am. Ceram. Soc. 81 (1998) 2023–2028.
[10] T. Ikegami, T. Mori, Y. Yajima, S. Takenouchi, T. Misawa, Y. Moriyoshi, J. Ceram. Soc. Jpn. 107 (1999) 297–299.
[11] T. Ikegami, J.-G. Li, T. Mori, Y. Moriyoshi, J. Am. Ceram. Soc. 85 (2002) 1725–1729.
[12] J.-G. Li, T. Ikegami, J.-H. Lee, T. Mori, J. Am. Ceram. Soc. 83 (2000) 961–963.
[13] Y. Zhang, H. Yu, Ceram. Int. 35 (2009) 2077–2081.
[14] J.-G. Li, T. Ikegami, T. Mori, J. Am. Ceram. Soc. 88 (2005) 817–821.
[15] K. Nakanishi, P.H. Solomon, Infrared Absorption Spectroscopy, Holden Day, San Francisco, 1977.
[16] T. Ikegami, Y. Mori, M. Matsuda, H. Suzuki, Yogyo Kyokaishi 81 (1973) 379–382.
[17] N.L. Smirnova, N.V. Akimova, N.V. Belov, J. Struct. Chem. 8 (1967) 65–68.